Arch. Metall. Mater. **70** (2025), 1, 405-414

DOI: https://doi.org/10.24425/amm.2025.152559

D. SZELIGA[1], J. FORYŚ[1*], J. KUSIAK[1], R. KUZIAK[2],
R. NADOLSKI[1], M. PIETRZYK[1], Ł. RAUCH[1]

UNCERTAINTY AND STOCHASTICITY IN MODELLING OF MICROSTRUCTURE EVOLUTION DURING HOT ROLLING OF STEELS

Advanced numerical models, which predict heterogeneity of microstructural features, are needed to design modern steels with heterogeneous microstructures. Models based on stochastic internal variables meet this requirement. Our stochastic model accounts for the random character of the recrystallization and transfers this randomness into equations describing the evolution of the dislocation populations and the grain size during the hot deformation of steels. The idea of the internal variable model, with the dislocation density and the grain size being stochastic variables, is described in the paper. The material parameters, which influence accuracy and reliability of the model, were identified. They compose shear modulus, lattice friction stress and the mean free pass for dislocations. Numerical test showing influence of these parameters on the identification of the model coefficients were performed and a hint how these parameters should be selected is given. Compression loads and histograms of the grain size measured in the experimental compression tests were used to identify the coefficients in the model. The model was applied to simulations of the industrial process of the hot strip rolling. It was shown that the model can be used to both predictions of the microstructural heterogeneity caused by the stochastic character of microstructure evolution and to the evaluation of the uncertainty of phase composition in the final product. The latter is due to the uncertainty of the boundary conditions.

Keywords: Stochastic model; microstructure evolution; heterogeneity; uncertainty; hot rolling

Introduction

Continuous development of the industry is associated with the search for new construction materials that combine high strength with good formability and a high strength-to-density ratio. Steels have met these requirements for many decades. Historically, the grain refinement was the main strengthening mechanism for steels investigated during the second half of the 20th century, when High Strength Low Alloyed (HSLA) steels were developed [1]. By controlling the precipitation and its influence on the recrystallization, an improvement of the strength and workability was obtained [2]. Different strengthening mechanism was used in the Advanced High Strength Steels (AHSS), which were developed in the last decades of the 20th century. These steels are composed of soft ferrite matrix with hard islands of bainite, martensite and retained austenite. The AHSSs benefit from the best features of the phases they are made of [3,4]. Among AHSSs, Dual Phase (DP) and Complex Phase (CP) steels are the two most widely used in car body applications [5]. The correlation between mechanical properties and microstructure of these steels has been extensively studied. In general, DP steels combine high strength with large total elongation, but their local formability is low, what is caused by sharp gradients of properties at interfaces. Multiphase CP steels with smoother gradients are much better in stretch applications. It has been shown that the microstructural heterogeneity exists in multiphase steels and directly influences local mechanical properties [3], but the exact correlation between microstructural heterogeneity and mechanical properties of CP steels is yet difficult to quantify. Advanced numerical models are needed to gain knowledge on distributions of microstructural features and to design thermal-mechanical cycles allowing to obtain moderate gradients of properties. These models should predict distributions of various microstructural parameters instead of their average values. Beyond this, since optimization is the prospective application of these models, they must be characterized by low computing costs.

Beyond predictions of the microstructure heterogeneity, a problem of the uncertainty of predictions is also important [6].

[1] AGH UNIVERSITY OF SCIENCE AND TECHNOLOGY, FACULTY OF METALS ENGINEERING AND INDUSTRIAL COMPUTER SCIENCE, AL. MICKIEWICZA 30, 30-059 KRAKÓW, POLAND
[2] RESEARCH GROUP PROCESSES SIMULATION, UPPER-SILESIAN INSTITUTE OF TECHNOLOGY, UL. K. MIARKI 12-14, 44-100 GLIWICE, POLAND

* Corresponding author: jakubforys@agh.edu.pl

Knowledge of the possible spread of the predicted target values, such as microstructural parameters, is needed for a reliable process design. In production, the spread of product properties is due to uncertainties in the processing conditions and the material composition.

Thus, the objectives of the work were twofold. The first objective was to apply the fast mean-field stochastic model with extended predictive capabilities to simulation of the hot forming and cooling of steels. As it was shown in [7], the description of the heterogeneous microstructure of metals and alloys using internal stochastic variables allows for building the mean-field model with the capability to predict gradients of product properties. The same stochastic model can also be used to evaluate the uncertainty of the predictions of microstructural parameters when the uncertainty of the boundary conditions (temperatures) is known. This was the second objective of the paper.

1. Model

The internal variable stochastic model for hot deformation was proposed in our earlier publication [8]. The model was identified based on the experimental data [7]. In publication [9] the model was applied to simulations of multistep hot forming processes. The details of the model are presented in [8] and only main equations are repeated below for the completeness of the publication.

1.1. Main equations

The hot deformation model is based on the fundamental works of Kocks, Estrin and Mecking (so called KEM model) [10,11]. The KEM model follows the Taylor theory [12] and assumes that evolution of the dislocation population determines the flow stress during the plastic deformation. The mean free path for dislocations l is the main parameter which controls hardening. This path is a distance travelled by a dislocation segment before it is locked by interaction with the microstructure. In his primary work Taylor made following assumptions: i) the mean free path of mobile dislocations does not depend on strain and temperature, ii) no dynamic recovery takes place, iii) the grown-in dislocation density ρ_0 can be neglected, iv) the plastic deformation is homogeneous. By proceeding from these assumptions, when the dislocation line moves, it produces a shear strain $d\varepsilon$. The stored density has then statistically increased with the storage rate $d\rho/d\varepsilon = 1/bl$, where b is the module of the Burgers vector. This definition is only valid in differential form, as dislocation lines multiply when they move.

The Taylor's theory was further developed by Bergström [13] (see also review in [14]), who introduced softening due to dynamic recovery, which, in accordance with the law of natural decay, is proportional to the total dislocation density, $\rho(\varepsilon)$. The rate at which dislocations are re-mobilized or annihilated is therefore proportional to the product $A_2\rho(\varepsilon)$, where A_2 is the strain-independent material constant representing the remobilization dynamic recovery coefficient. It was also assumed that the recovery process is mainly based on re-mobilization, at least for metals with high stacking fault energy (SFE) and many glide systems, e.g. soft steel.

Since the flow stress during plastic deformation is governed by the evolution of dislocations populations, a competition of storage and annihilation of dislocations, which superimpose in an additive manner, controls a hardening. If in accordance with Taylor the rate by which dislocations are generated is proportional to $1/(bl)$, then the rate by which the dislocation density increases is written as:

$$\rho' = (A_1 - A_2\rho)\dot{\varepsilon} \tag{1}$$

Coefficients A_1 and A_2 responsible for hardening and recovery are:

$$A_1 = \frac{1}{bl} \qquad A_2 = a_2\dot{\varepsilon}^{a_8}\exp\left(\frac{-a_3}{RT}\right) \tag{2}$$

where: b – Burgers vector, l – mean free path for dislocations, T – temperature in K, a_3 – activation energy for self-diffusion, which is a state variable, a_8 – coefficient.

Eq. (1) is the simplest form of the model based on the evolution of dislocation populations. Advanced models have been developed during last few decades. Various types of dislocations were considered [15] and various mechanisms of the recovery were introduced [16]. However, since the solution of the evolution equation for the stochastic variables is time-consuming, we decided to build the model based on the simple Eq. (1) and we focused on the analysis of the influence of various material parameters on the accuracy and the reliability of the model. This part is described in the Section 2.2.

In the deterministic solution of the evolution equation, the recrystallization is introduced following publication [17]. The idea of the numerical implementation of the model is described in [18] and the mathematical background is discussed in [19]. In publication [8] the critical time for the dynamic recrystallization was substituted by a random character of the recrystallization. Thus, the evolution of the dislocation density is governed by the following equation written in the incremental form:

$$\begin{aligned}\rho(t_i) &= \rho(t_0)\left[1-\xi(t_i)\right]+\\ &+\left\{\rho(t_{i-1})+\left[A_1\dot{\varepsilon}-A_2\rho(t_{i-1})\dot{\varepsilon}^{1-a_7}\right]\Delta t\right\}\xi(t_i)\end{aligned} \tag{3}$$

where: t – time, $\dot{\varepsilon}$ – strain rate, a_7 – coefficient, which accounts for the effect of the strain rate on the dynamic recovery.

The parameter $\xi(t_i)$, accounts for a random character of the recrystallization and its distribution is described by the conditions:

$$\begin{aligned}\mathbf{P}\left[\xi(t_i)=0\right] &= \begin{cases} p(t_i) & \text{if } p(t_i)<1 \\ 1 & \textit{otherwise}\end{cases}\\ \mathbf{P}\left[\xi(t_i)=1\right] &= 1-\mathbf{P}\left[\xi(t_i)=0\right]\end{aligned} \tag{4}$$

In Eq. (4), $p(t_i)$ is a function that bounds together the probability that the material point recrystallizes in a current time step and the present state of the material:

$$p\left(t_i\right) = a_4 \rho\left(t_{i-1}\right)^{a_6} \frac{3\gamma\left(t_i\right)\tau}{D\left(t_{i-1}\right)} \exp\left(\frac{-a_5}{RT}\right)\left(1 - X\left(t_{i-1}\right)\right)\Delta t \tag{5}$$

where: D – grain size in mm, τ – energy per unit dislocation length, X – recrystallized volume fraction, a_4, a_5, a_6, a_{17} – coefficients.

Comparing to the model in [8,9], multiplication by the term $(1 - X(t_{i-1}))$ was added in the Eq. (5). It means that non-Poissonian probability of the nucleation was applied. In this approach, progress of the recrystallization involves a decrease of that probability. Recrystallized volume fraction $X(t_{i-1})$ is calculated from the number of points, for which parameter $\xi(t)$ in the time $[0 - t_{i-1}]$ was zero:

$$X\left(t_{i-1}\right) = \frac{N_X}{N} \tag{6}$$

where: N_X – number of points for which in previous time steps parameter $\xi(t_i)$ was zero, what means that recrystallization occurred for this point, N – number of the Monte Carlo points.

In Eq. (4), coefficient γ represents a migrating grain boundary area per unit volume as a function of the recrystallized fraction. Following [17], we assumed that γ depends on the distribution of $\xi(t_{i-1})$ in the previous step, see [8]. The model was extended in work [9] by including the interpass times and the static phenomena in the simulations.

The Eq. (1) was solved using Monte Carlo method. Many trajectories were calculated for the randomly generated values of $\rho(t_0)$ and $D(t_0)$. The results were aggregated into histograms at consecutive time steps t_i. We start with the grain size $D(t_0) \equiv D_0$, which is a random variable described by the Weibull distribution. Based on the measured grain size distributions shown in [7] the shape parameter equal to 10 was assumed. The scale parameter $\bar{D}_0$ was established as the average grain size measured after preheating before deformation. When during the calculation, the random parameter $\xi(t_i) = 0$, the considered point recrystallizes and its new grain size $D(t_i)$ is drawn from the Gauss distribution with the standard deviation being an optimization variable a_{22} in the model. The expected value of the grain size is either dynamically (for $\dot{\varepsilon} > 0$) or statically (for $\dot{\varepsilon} = 0$) recrystallized grain size. See [9] for the description, how histograms of the austenite grain size are calculated.

Beyond the histograms of the selected parameters, the model calculates the average dislocation density ρ_{av} and further the flow stress σ_p, as follows:

$$\sigma_p = \sigma_0 + a_{23} M b G \sqrt{\rho_{av}} \qquad \rho_{av} = \frac{1}{Np}\sum_{i=1}^{Np} \rho_i \tag{7}$$

where: σ_0 – the stress due to lattice friction, M – Taylor factor, G – shear modulus, b – a module of the Burgers vector, Np – number of points in the Monte Carlo solution, ρ_i – dislocation density for the Monte Carlo point i, a_{23} – coefficient.

Calculations of the flow stress will be used in the next section to determine the loads in the compression tests and, further, will be a part of the objective function in the identification of the coefficients in the model.

2. Identification, validation and numerical tests of the model

2.1. Objective function

The whole stochastic model contains 25 coefficients, which are grouped in the vector **a**. These coefficients were identified based on the experimental data. The experiments composed compression tests for asymmetrical samples performed at various temperatures and strain rates [20]. The material was unalloyed, low-carbon, welded structural steel S355J2 containing 0.12%C and 1.3%Mn. Inverse analysis was used to find the coefficients in the model. Compression loads and histograms of the austenite grain size were measured in the experiments. Inverse analysis was transferred into the optimization task and coefficients **a** were determined by searching for the minimum of the following objective function:

$$\Phi(\mathbf{a}) = d\left(y_c(\mathbf{a}), y_m\right) + d\left(H_c\left(\mathbf{a}\right), H_m\right) \tag{8}$$

where: $y_c(\mathbf{a})$ – average dislocation density calculated for the model coefficients **a**, y_m – dislocation density calculated for the measured loads in the experimental tests, d – metric in the output space Y.

The first term in Eq. (8) is the Root Mean Squared Error (RMSE) between measured and calculated dislocation density. Measurement of the dislocation density in situ during hot forming is not possible. Therefore, dislocation density was determined indirectly from the measurements of the compression loads. However, the loads measured in the experiments are influenced by the friction between the die and the sample, the barrelling of the sample and the deformation heating. Inverse analysis allows to eliminate these effects and to calculate the flow stress as a function of the temperature and the strain rate, see [21]. Following this, Eq. (7) was used to calculate the dislocation density and to compare it with the predictions of the stochastic model. The second term in Eq. (8) represents the distance between the measured and calculated histograms of the grain size. The Bhattacharyya metric was used to calculate this distance, see [8] for details.

2.2. Numerical tests

Let us now discuss and analyse those parameters in the stochastic model, selection of which is important for the reli-

ability of the inverse analysis. The mean free path for dislocations l is the main parameter, which may significantly influence the identification of the model. As it is seen in Eq. (2), l controls the rate of the increase of the dislocation density due to hardening. Very little is presently known about the way the mean free path l depends on dislocation interactions, stress, and specimen orientation. The most important contribution to the mean free paths arises from the interactions of the moving dislocations with "forest" dislocations (that is, dislocations of other systems that pierce their slip plane) and their subsequent storage. As it has been mentioned, the Taylor's theory [12] and primary work of Bergström [13] assume that the mean free path l is strain and temperature independent.

In his further works Bergström assumed that the mean free path l decreases with progress of plastic deformation [14]. Such a behaviour is mathematically described as follows:

$$\frac{dl}{d\varepsilon} = k_l\left[l(\varepsilon) - l_0\right] \tag{9}$$

After integration we obtain:

$$l(\varepsilon) = l_0 + (l_1 - l_0)\exp(-k_l\varepsilon) \tag{10}$$

where: ε – strain, l_0, l_1 – initial and final values of l, respectively.

The Bergström approach is well described in [14]. In that publication, initial and final values of the mean free path l are determined by fitting to the experimental results. Decrease of the mean free path with increasing strain was observed by many researchers and they introduced relations either $l \sim \varepsilon^{-0.5}$ or $l \sim \rho^{-0.5}$, see e.g. [22]. In a majority of the published works the latter is considered:

$$l = \frac{a_2}{\sqrt{\rho}} \tag{11}$$

In some papers the effect of the grain size is introduced and the mean free path is calculated as [23]:

$$\frac{1}{l} = \frac{1}{a_1 D} + \frac{\rho^c}{a_2} \tag{12}$$

In a majority of publications, Eq. (12) is used directly with c = 0.5. However, Some researchers substituted power –0.5 by a variable c ($l \sim \rho^{-c}$), which during deformation decreases from 0.5 to 0 [24,25]. This is based on the assumption that with increasing dislocation density, the cells retain their shape but decrease in size. For larger strains the cell diameter becomes constant: $c = 0$. So, c is a parameter between 0 and 0.5 with a fit coefficient c_1, according to the following equation:

$$c = 0.5\exp(-c_1\varepsilon) \tag{13}$$

The same effect was obtained in publication [26] by adding a minimum size of the cell $l_{\min}$ to Eq. (12):

$$\frac{1}{l(\varepsilon)} = \frac{1}{a_1 D} + \frac{\rho^c}{a_2} + \frac{1}{l_{\min}} \tag{14}$$

Neither Eq. (13) nor Eq. (14) were investigated in our project. More complex models of the mean free path l were proposed in [27,28].

As far as the effect of the temperature is considered, σ in Eq. (7) contains shear modulus, which is the temperature dependent, see discussion below. Although other parameters in the hardening part are assumed a-thermal, there are few publications in which the mean free path of dislocations is equal to the subgrain size which, in turn, depends on the Zener-Hollomon parameter Z. It introduces temperature dependence into the hardening term. In our earlier publication [8] we used the following equation:

$$l = a_1 Z^{-a_2} \tag{15}$$

In Eqs. (11)-(15) a_1 and a_2 are the coefficients, which are determined using inverse analysis. Values of these coefficients are different for different equations describing l.

It is seen from referenced research that the present knowledge about the mean free path of dislocations is limited and determination of coefficients in equations by fitting to experimental data is a common approach [14]. In our project we considered four models of the mean free path of dislocation and we identified coefficients in the whole stochastic model by the inverse analysis for the results of compression tests. The identification of the model was performed for the following equations describing the mean free path: i) The mean free path is an optimization variable $l = a_1$, ii) Eq. (11), iii) Eq. (12), iv) Eq. (15). The final values of the objective function (8) after identification are presented in Fig. 1. It is seen that these values do not differ noticeably, what means the inverse analysis is capable to find coefficients of the stochastic model, which give good results for different models of the mean free path of dislocations. In all further simulations in this paper Eq. (12) was used.

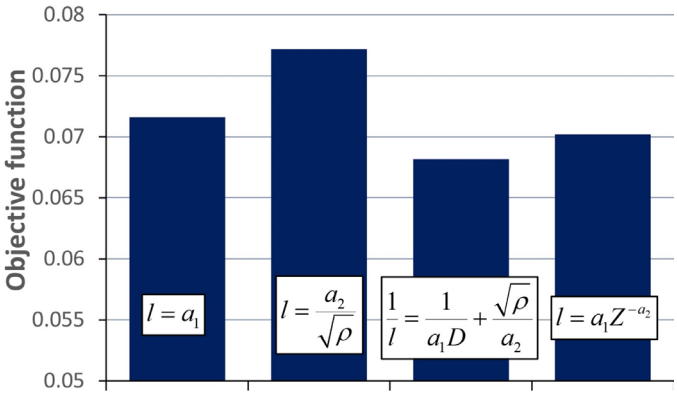

Fig. 1. The final values of the objective function (8) after model identification for different equations describing the mean free path for dislocations

The lattice friction stress σ_0 in Eq. (7) is another parameter, which is not defined precisely in the models published by various researchers. Generally, in discussions on the lattice friction stress a reference to the Hall-Petch (HP law) is made. In our solution we assumed that σ_0 is identified in the inverse approach and it is coefficient a_{24} in the vector of the state variable.

In Eq. (7), which is used to calculate the dislocation density from the measured flow stress, Taylor factor $M = 3.1$ and a module of the Burgers vector $b = 2.5\times10^{-10}$ m are established values. Coefficient a_{23} is a state variable in the optimisation procedure and it is determined by searching for the minimum of the objective function (8). In means that the shear modulus is an important parameter, which controls the inverse analysis and can be a source of the errors. The knowledge of the relation of this modulus on the temperature is necessary to compare measured flow stress with that calculated by the model. Thus, the shear modulus is another parameters, which strongly influence the inverse analysis and a proper selection of this modulus is crucial for the accuracy of the identification procedure.

Many papers dealing with the relation of the shear modulus on the temperature were published and large spread of the published data can be observed. First experiments aiming at the evaluation of the elastic moduli ware performed more than a hundred years ago [29]. Typically, the method for measuring elastic modulus at temperature is from the stress–strain relation obtained from a tensile test. The accuracy of this technique is limited by rate of loading, deformation effects such as creep and the stress level at which the elastic properties are determined. Further, the complexity of the experimental arrangement leads to difficulties in measuring the strain on the material [30]. An alternative is the impulse excitation technique (IET), which is a non-destructive, easy and fast method for characterization of elastic and acoustic properties of materials [31]. Therefore, in our analysis we focused only on the recent publications, assuming that better equipment was used to measure the modulus. Reported values of the shear modulus in the temperatures 900-1000°C (final stage of the hot forming of steels) vary from 7700-4000 MPa [32] to as large as 20000-16000 MPa. Authors of [33] investigated the steel S355J2, which is a subject of measurements in the present work, and they reported even lower values of 5500-3650 MPa. Some researchers measured shear modulus in the temperatures below 800°C and extrapolation of their results to higher temperatures is uncertain [34]. For example, in the paper [30] G was measured in the temperatures up to 723°C, but the extrapolation to the temperature range 900-1000°C gives as large values as 59200-56500 MPa. Several publications show that in the temperatures above 800°C drop of the shear modulus with an increase of the temperature is smaller and the curve is less steep. A thorough review of various measurements of the shear modulus is presented in the NIST report [35]. Selected results of calculations of the shear modulus based on various publications are also presented in Fig. 2. Maximum and minimum values reported in [35] are marked with dashed line in this figure. Having all these data in mind, we have proposed approximation of the $G(T)$ relationship by the function proposed in [32]:

$$G = G_0\left\{\begin{array}{l} b_1\exp\left[-\left(\dfrac{T-b_2}{b_3}\right)^2\right]+ \\ +\ c_1\exp\left[-\left(\dfrac{T-c_2}{c_3}\right)^2\right] \end{array}\right\} \qquad (16)$$

where: T – temperature in °C, D – grain size, G – shear modulus, G_0 – shear modulus in the room temperature, which for the investigated steel is 80200 MPa, b_1, b_2, b_3, c_1, c_2, c_3 – coefficients.

Coefficients b_1, b_2, b_3, c_1, c_2 and c_3 appearing in Eq. (16) were determined in [32] by approximation of the experimental data for a variety of steels and they are given in TABLE 1. The authors of [32] focused on the behaviour of steels in the conditions of the fire and the majority of the investigated steels was in the quenched condition. In the present work, to make the results closer to the conditions of hot deformation, coefficient c_2 was slightly modified. This modification does not allow to drop $G(T)$ to very low values above 1000°C and, in consequence, changes of the shear modulus in the temperature range 900-1100°C were closer to that reported in [35] for typical construction steels. A plot of the function (16) is presented in Fig. 2 by a thick black line.

TABLE 1

Coefficients in Eq. (16) for the investigated steel

b_1	b_2, °C	b_3, °C	c_1	c_2, °C	c_3, °C
0.1871	–12.96	132	0.9199	181.6	770

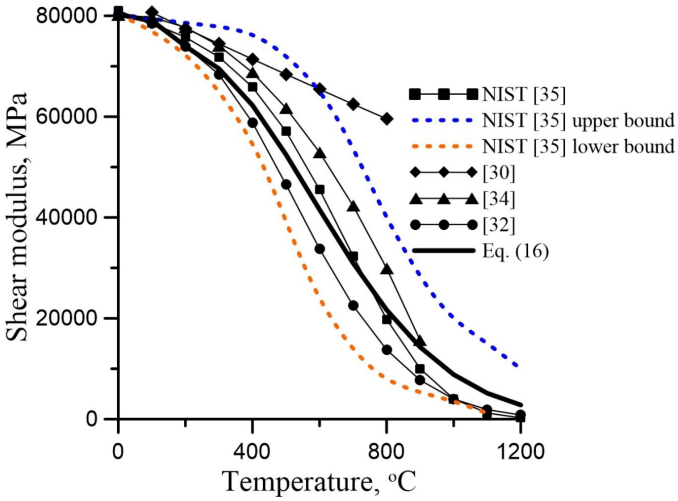

Fig. 2. Selected examples of calculations of the shear modulus based on various publications

Recapitulating, identification of the model was performed assuming that:

- Eq. (12) describes the mean free path for dislocations.
- The lattice friction stress σ_0 in Eq. (7) is identified in the inverse approach and it is a_{23} in the vector of the state variables
- The shear modulus is a function of the temperature and it is described by Eq. (16).

2.3. Verification of the model

The model with the coefficients determined by searching for the minimum of the objective function (8) was verified. A full set

of the results of the comparison between measured and calculated histograms of the austenite grain size is shown in [20]. Good agreement between measurements and predictions was obtained for grain size distributions right after deformation (dynamic recrystallization) and at different times after the deformation (static recrystallization). The Bhattacharyya metric, which was selected in [20] as a measure of the distance between the two histograms, did not exceed 0.1, which is a very good result for the comparison of the microstructures.

Analysis of the measured compression loads have shown that the effect of the austenite grain size prior to deformation is negligible [20]. Results of the comparison of the measured and calculated flow stress are shown in Fig. 3. The measured flow stress was obtained by the inverse analysis [21] for the loads, which were measured in the compression tests. The calculated flow stress was obtained from Eq. (7) for an average dislocation density predicted by the stochastic model. It is seen that acceptable agreement between measured and calculated parameters was obtained. Recapitulating, the verification confirmed model's good predictive capabilities. It was assumed that the model will give realistic results of simulations of the industrial process described in Chapter 3.

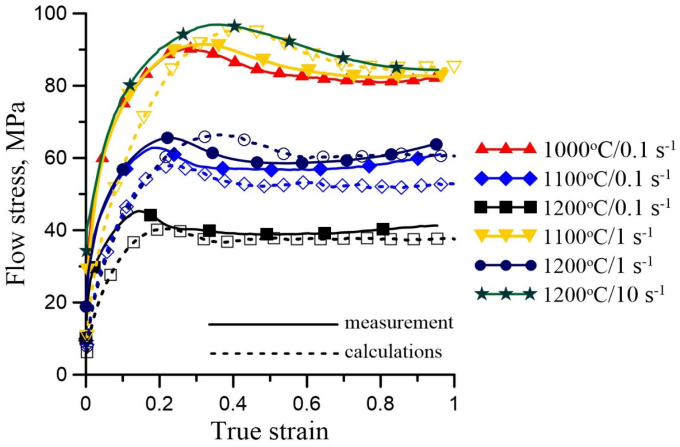

Fig. 3. Comparison of the measured and calculated flow stress

3. Case study

The hot strip mill composed of the reverse roughing mill, 6-stand continuous finishing mill and 2-section laminar cooling was considered. Rolling of the steel strip measuring 1500×4 mm was simulated and the selected results for the finishing mill and the laminar cooling are presented below. The work roll radius was 450 mm in all stands and the distance between stands was 5.8 m. The rolling schedule was 40 → 19.2 → 12.6 → 9.3 → 6.9 → 5.2 → 4 mm. The strip velocity at the exit from the last stand was v_6 = 6.8 m/s. Classical hot strip rolling with the end of the rolling temperature of about 940°C was simulated. After exit from the last stand the strip enters the laminar cooling system and phase transformations are simulated. Since the hot rolling model predicted full recrystallization at the temperature A_{e3}, the model for recrystallized material was applied to simulate phase transformations. The distributions of the grain size calculated by the hot rolling model were used as an input for simulations of phase transformations.

3.1. Heterogeneous microstructure

Monte Carlo solution with 20000 points was used to calculate distributions of the dislocation density and the austenite grain size during rolling accounting for the random character of the recrystallization, following Eqs. (4) and (5). In-house finite element (FE) program [36] was used to calculate strains, strain rates, stresses and temperatures during rolling. The stochastic model describing evolution of dislocations and grain size was solved along the flow lines in the roll gap using current, local values of the strain rate and the temperature calculated by the FE program. Calculated strains in subsequent passes and changes of the average dislocation density during hot strip rolling and between the exit from the last stand and the beginning of the laminar cooling are presented in Fig. 4. It is seen, that due to large strains and high temperature, recrystallization is completed during intervals in the first three passes. Calculated histograms (10 bins each) of distributions of the dislocation density and the austenite grain size are shown in Fig. 5 for the passes 4, 5 and 6. It is seen that there is no dynamic recrystallization in these passes, which is due to high strain rates and reasonably low temperature. The static recrystallization is completed after pass 4. Partial recrystallization was predicted between passes 5 and 6, with about 50% of the SRX. Anyway, as it has been mentioned, the material was fully recrystallized at the beginning of the phase transformations.

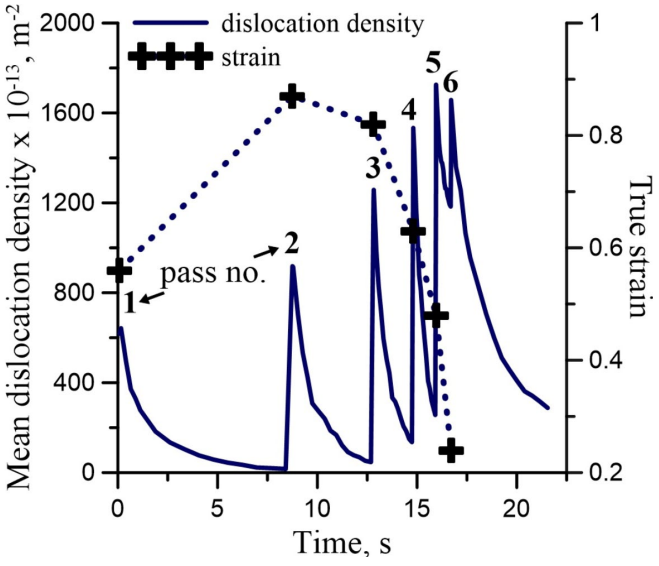

Fig. 4. Calculated strains in subsequent passes and changes of the average dislocation density during hot strip rolling and between the exit from the last stand and the beginning of the laminar cooling

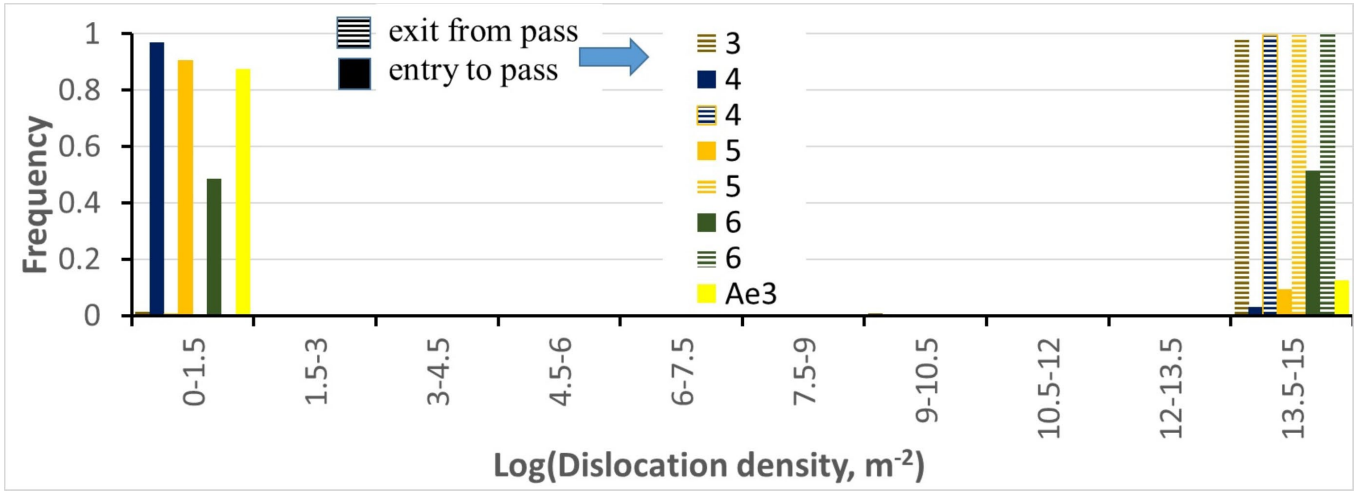

a)

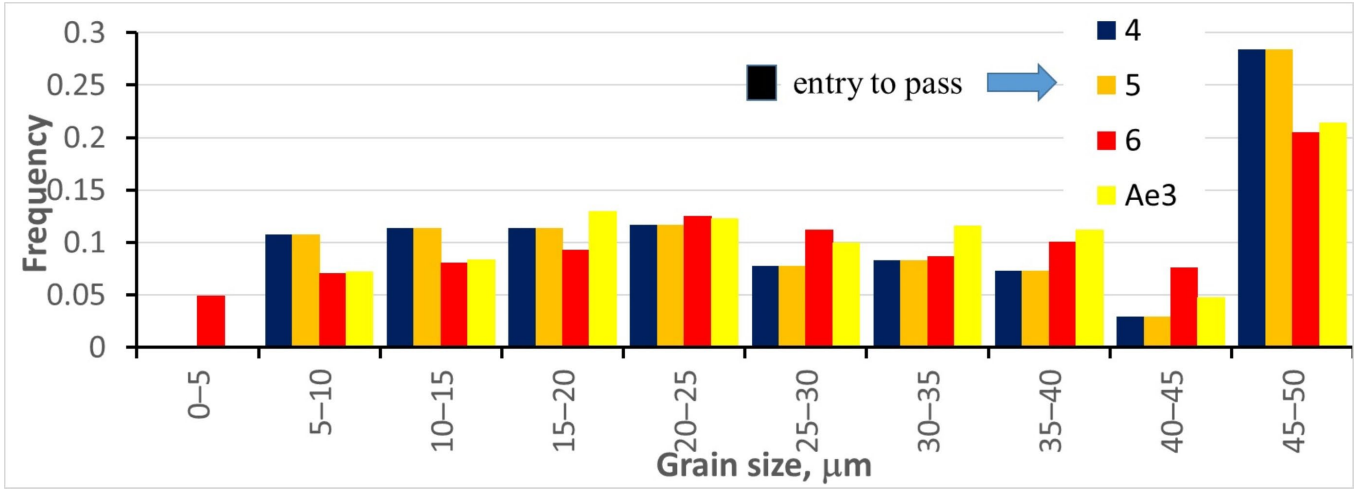

b)

Fig. 5. Calculated histograms for the dislocation density (a) and grain size (b) during and after the hot deformation calculated using the stochastic model

3.2. Cooling and phase transformation model

A typical system of laminar cooling after hot strip rolling [37] was considered as an example of practical application of the model. The system is composed of two sections divided in 4 zones. There are 40 boxes 1 m long in each section. The distance between the sections is 20 m. Cooling conditions, which compose water flux in various zones and the heat transfer coefficient corresponding to this flux, are given in [37]. The finite element model of the laminar cooling and coiling processes is described in that paper, as well. Rolling velocity in the last stand v_6, strip thickness h_6, and finishing rolling temperature T_f have been considered as independent variables. The calculated histogram of the grain size at the beginning of phase transformations (Fig. 5b) was an input for simulations. Phase transformation model and coefficients in this model for the investigated steel are described in [20] and they are not repeated here because of the limited space.

Simulations of the laminar cooling assuming determined boundary conditions and average grain size prior to transformation equal 29.6 mm (average for the histogram in Fig. 5b) predicted 76.3% of ferrite, 22.2% of pearlite and a negligible amount of the bainite.

3.3. Heterogeneity of the microstructure and uncertainty of the predictions

In the following calculations, the grain size histogram shown in Fig. 5b was used as the input for simulations of the laminar cooling. Beyond this, the uncertainty of the boundary conditions was accounted for. The temperature at the entry to the cooling section was considered as the first source of the uncertainty. This was done in a qualitative manner only. Due to a lack of the satisfactory large data set necessary for the statistical analysis, a Gauss distribution of the entry temperature with the standard deviation of 10°C was assumed on the basis of measurements in one of the hot strip mills. The boundary conditions during cooling were considered as the second source of the uncertainty. These boundary conditions are represented

by the heat transfer coefficient (*HTC*), which depends on the water flux in subsequent boxes of the laminar cooling, see [37] for details. Again, due to a lack of the satisfactory large data set, we assumed that the *HTC* during laminar cooling is given by the Gauss distribution:

$$f\left(HTC\right)=\frac{1}{\sqrt{2\pi\sigma^2}}\exp\left[-\frac{\left(HTC-\bar{\bar{HTC}}\right)^2}{2\sigma^2}\right] \qquad (17)$$

where: $\bar{\bar{HTC}}$ – the expected value of the heat transfer coefficient calculated following the model in [37], σ – standard deviation, assumed 50 W/m^{2}K.

Since the input data for the phase transformation model were stochastic and the model itself is stochastic, the calculated ferrite grain size and phase composition were obtained in the form of histograms.

Histogram of the ferrite grain size after cooling is shown in Fig. 6. This histogram was obtained assuming that boundary conditions were fixed (not disturbed). It means that this histogram represents heterogeneity of the microstructure, which is due to the heterogeneity of the microstructure after hot rolling and to the stochastic character of the phase transformation model.

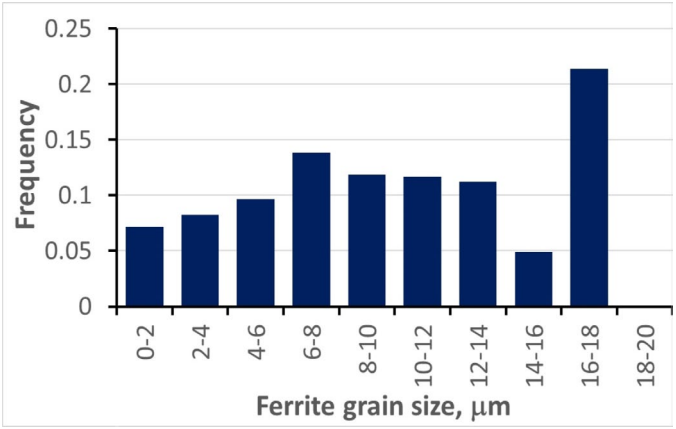

Fig. 6. Calculated histograms of the ferrite grain size after cooling

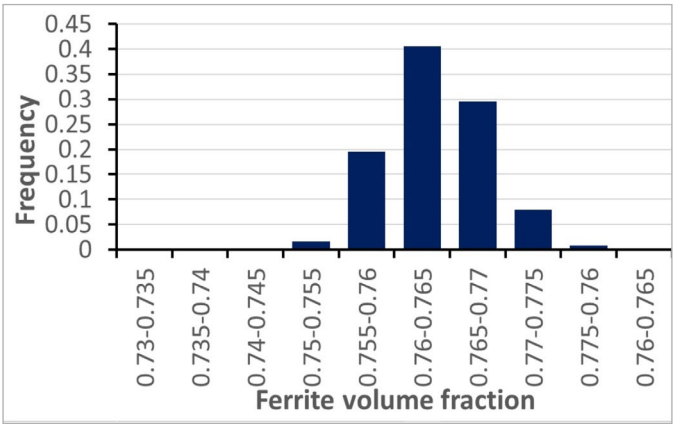

Fig. 7. Calculated histograms of the phase composition after cooling

The histogram of the ferrite volume fraction after cooling is shown in Fig. 7. This distribution is due to the heterogeneity of the microstructure prior to transformation and to the uncertainty of the boundary conditions. Since properties of product depend on the phase composition of steel, the model can be further used to predict uncertainty of the properties due to uncertainty of the process parameters. It is seen in Fig. 7, however, that small standard deviation assumed in this paper for the entry temperature and for the heat transfer coefficient resulted in small variations of the phase composition.

4. Conclusions

The stochastic model describing the evolution of the microstructure during hot strip rolling and laminar cooling is presented in the paper. Selection of proper parameters in the evolution of dislocations equation is crucial for the accuracy of simulations. Numerical tests were performed to evaluate the effect of the mean free path of dislocation, the lattice friction stress and shear modulus. The following conclusions were drawn:

- Inverse calculations and identification of the model were performed for different equations describing the mean free path of dislocations. The final values of the objective function obtained for various equations were comparable. It means that inverse method is flexible. It allowed to fit the coefficients to various free path equations and good results were obtained.
- Quantitative evaluation of the friction stress in Eq. (7) is difficult. Therefore, this stress was introduced as a state variable in the inverse analysis.
- Identification based on the inverse analysis for the compression tests yielded coefficients in the model, which give good agreement between measurements and predictions of both average values and distributions of selected parameters.

Remaining conclusions:

- Capability to predict histograms of microstructural features instead of their average values is the main advantage of the model.
- Capability to assess the effect of different material parameters (l, G, σ_0) on the variability of the predicted microstructure of the final product.
- The model was applied to simulations of the industrial hot strip rolling. The results agree with our knowledge about this process, confirming the model's capability to support the optimal rolling technology design.
- The deterministic simulation of the laminar cooling showed that the sequence of the fast/slow/fast cooling allows to obtain of a DP microstructure.
- The stochastic phase transformation model can account for the random character of the input (grain size) and boundary conditions (*HTC*). In consequence, the heterogeneity of the microstructure (ferrite grain size) and the uncertainty of the predictions of the phase composition could be evaluated.

- In the hot deformation part, the model is completed and, when coupled with the finite element program, can be applied to any hot forming process. The phase transformations part is still a work in progress.

Acknowledgements

Financial assistance of the National Science Foundation in Poland (NCN), project no. 2021/43/B/ST8/01710, is acknowledged.

REFERENCES

[1] T. Gladman, The physical metallurgy of microalloyed steels. The Institute of Materials (1997).

[2] N. Isasti, D. Jorge-Badiola, M.L. Taheri, P. Uranga, Microstructural and precipitation characterization in Nb-Mo microalloyed steels: estimation of the contributions to the strength. Metals and Materials International **20**, 807-817 (2014).

[3] Y. Chang, M. Lin, U. Hangen, S. Richter, C. Haase, W. Bleck, Revealing the relation between microstructural heterogeneities and local mechanical properties of complex-phase steel by correlative electron microscopy and nanoindentation characterization. Materials and Design **203**, 109620 (2021).

[4] Y. Chang, C. Haase, D. Szeliga, Ł. Madej, U. Hangen, M. Pietrzyk, W. Bleck, Compositional heterogeneity in multiphase steels: characterization and influence on local properties. Materials Science and Engineering **A827**, 142078 (2021).

[5] M.K. Singh, Application of steel in automotive industry. International Journal of Emerging Technology and Advanced Engineering **6**, 246-253 (2016).

[6] T. Henke, M. Bambach, G. Hirt, Quantification of uncertainties in grain size predictions of a microstructure-based flow stress model and application to gear wheel forging. CIRP Annals – Manufacturing Technology **62** (1), 287-290 (2013).

[7] D. Szeliga, N. Czyżewska, K. Klimczak, J. Kusiak, R. Kuziak, P. Morkisz, P. Oprocha, V. Pidvysotsk'yy, M. Pietrzyk, P. Przybyłowicz, Formulation, identification and validation of a stochastic internal variables model describing the evolution of metallic materials microstructure during hot forming. International Journal of Material Forming **15**, 53 (2022).

[8] K. Klimczak, P. Oprocha, J. Kusiak, D. Szeliga, P. Morkisz, P. Przybyłowicz, N. Czyżewska, M. Pietrzyk, Inverse problem in stochastic approach to modelling of microstructural parameters in metallic materials during processing. Mathematical Problems in Engineering (2022). Article ID 9690742. DOI: https://doi.org/10.1155/ 2022/9690742

[9] D. Szeliga, N. Czyżewska, K. Klimczak, J. Kusiak, R. Kuziak, P. Morkisz, P. Oprocha, M. Pietrzyk, Ł. Poloczek, P. Przybyłowicz, Stochastic model describing evolution of microstructural parameters during hot rolling of steel plates and strips. Archives of Civil and Mechanical Engineering **22**, 239 (2022). DOI: https://doi.org/10.1007/s43452-022-00460-2

[10] H. Mecking, U.F. Kocks, Kinetics of flow and strain-hardening. Acta Metallurgica **29**, 1865-1875 (1981).

[11] Y. Estrin, H. Mecking, A unified phenomenological description of work hardening and creep based on one-parameter models. Acta Metallurgica **32**, 57-70 (1984).

[12] G.I. Taylor, The mechanism of plastic deformation of crystals. Part I – Theoretical, Proc. of the Royal Society of London A: Mathematical, Physical and Engineering Sciences **145**, 362-387 (1934).

[13] Y. Bergström, The plastic deformation of metals – a dislocation model and its applicability. Reviews on Powder Metallurgy and Physical Ceramics **2** (2-3), 79-265 (1983).

[14] Y. Bergström, The plastic deformation process of metals – 50 years development of a dislocation based theory. A journey from homogeneous to inhomogeneous plastic deformation. Metalliska Material, paper 10 (2015).

[15] F. Roters, D. Raabe, G. Gottstein, Work hardening in heterogeneous alloys – a microstructural approach based on three internal state variables. Acta Materialia **48**, 4181-4189 (2000).

[16] P. Lisiecka-Graca, K. Bzowski, J. Majta, K. Muszka, A dislocation density-based model for the work hardening and softening behaviors upon stress reversal. Archives of Civil and Mechanical Engineering **21**, 84 (2021).

[17] R. Sandstrom, R. Lagneborg, A model for hot working occurring by recrystallization. Acta Metallurgica **23**, 387-398 (1975).

[18] C.H.J. Davies, Dynamics of the evolution of dislocation populations. Scripta Metallurgica et Materialia **30**, 349-353 (1994).

[19] N. Czyżewska, J. Kusiak, P. Morkisz, P. Oprocha, M. Pietrzyk, P. Przybyłowicz, Ł. Rauch, D. Szeliga, On mathematical aspects of evolution of dislocation density in metallic materials. IEEE Access **10**, 86793-86812 (2022).

[20] Ł. Poloczek, R. Kuziak, V. Pidvysotsk'yy, D. Szeliga, J. Kusiak, M. Pietrzyk, Physical and numerical simulations to predict distribution of microstructural features during thermomechanical processing of steels. Materials **15**, 1660 (2022).

[21] D. Szeliga, J. Gawąd, M. Pietrzyk, Inverse analysis for identification of rheological and friction models in metal forming. Computer Methods in Applied Mechanics and Engineering **195**, 6778-6798 (2006).

[22] G.Z. Voyiadjis, F.H. Abed, Effect of dislocation density evolution on the thermomechanical response of metals with different crystal structures at low and high strain rates and temperatures. Archives of Mechanics **57**, 299-343 (2005).

[23] J.M. Rodríguez, S. Larsson, J.M. Carbonell, P. Jonsén, Dislocation density based flow stress model applied to the PFEM simulation of orthogonal cutting processes of Ti-6Al-4V. Materials **13**, 1979 (2020). DOI: https://doi.org/10.3390/ma13081979

[24] E. Atzema, H. Mulder, Temperature dependence of steel constitutive behavior: a simplified model. Procedia Manufacturing **47**, 541-546 (2020).

[25] H. Vegter, H. Mulder, P. van Liempt, J. Heijne, Work hardening descriptions in simulation of sheet metal forming tailored to material type and processing. International Journal of Plasticity **80**, 204-221 (2016).

[26] D. Wedberg, Dislocation density based material model applied in FE-simulation of metal cutting. Licentiate thesis, Luleå University of Technology (2010).

[27] B. Devincre, T. Hoc, L. Kubin, Dislocation mean free paths and strain hardening of crystals. Science **320**, 1745-1748 (2008). DOI: https://doi.org/10.1126/science.1156101.

[28] K. Sedighiani, K. Traka, F. Roters, D. Raabe, J. Sietsma, M. Diehl, Determination and analysis of the constitutive parameters of temperature-dependent dislocation-density-based crystal plasticity models. Mechanics of Materials **164**, 104117 (2022).

[29] B. Hopkinson, F. Rogers, The elastic properties of steel at high temperatures. Proceeding of the Royal Society A, Mathematical, Physical and Engineering Sciences **76** (512), 419-425 (1905).

[30] B.A. Latella, S.R. Humphries, Young's modulus of a 2.25Cr–1Mo steel at elevated temperature. Scripta Materialia **51**, 635-639 (2004).

[31] I.I. Popov, M.V. Shitikova, Impulse excitation technique and its application for identification of material damping: an overview. IOP Conference Series: Materials Science and Engineering **962**, 022025 (2020).

[32] C. Maraveas, Z.C. Fasoulakis, K.D. Tsavdaridis, Mechanical properties of High and Very High Steel at elevated temperatures and after cooling down. Fire Science Reviews **6** (3), 1-13 (2017).

[33] J. Outinen, P. Mäkeläinen, Mechanical properties of structural steel at elevated temperatures and after cooling down. Second International Workshop Structures in Fire, Christchurch, 273-298 (2002).

[34] H. Ban, G. Zhou, H. Yu, Y. Shi, K. Liu, Mechanical properties and modelling of superior high-performance steel at elevated temperatures. Journal of Constructional Steel Research **176**, 106407 (2021).

[35] M. Seif, J. Main, J. Weigand, F. Sadek, L. Choe, C. Zhang, J. Gross, W. Luecke, D. McColskey, Temperature dependent material modeling for structural steels: formulation and application. In: Technical note 1907. National Institute of Standards and Technology (NIST) (2016).

[36] M. Pietrzyk, Through-process modelling of microstructure evolution in hot forming of steels. Journal of Materials Processing Technology **125-126**, 53-62 (2002).

[37] M. Pietrzyk, J. Kusiak, R. Kuziak, Ł. Madej, D. Szeliga, R. Gołąb Conventional and multiscale modelling of microstructure evolution during laminar cooling of DP steel strips. Metallurgical and Materials Transactions B **46B**, 497-506 (2014).